TUDelft

Delft University of Technology

Upgrading residues from wastewater and drinking water treatment plants as low-cost adsorbents to remove extracellular DNA and microorganisms carrying antibiotic resistance genes from treated effluents

Calderon Franco, D.; Apoorva, Seeram; Medema, G.J.; van Loosdrecht, Mark C.M.; Weissbrodt, D.G.

Important note
To cite this publication, please use the final published version (if applicable).
Please check the document version above.

Upgrading residues from wastewater and drinking water treatment plants as low-cost adsorbents to remove extracellular DNA and microorganisms carrying antibiotic resistance genes from treated effluents

David Calderón-Franco [a], Seeram Apoorva [a,1], Gertjan Medema [b,c], Mark C.M. van Loosdrecht [a], David G. Weissbrodt [a,*]

[a] Department of Biotechnology, Delft University of Technology, van der Maasweg 9, 2629 HZ Delft, the Netherlands
[b] KWR Watercycle Research Institute, Groningenhaven 7, 3433 PE Nieuwegein, the Netherlands
[c] Sanitary Engineering, Delft University of Technology, P.O. Box 5048, 2600 GA Delft, the Netherlands

HIGHLIGHTS

- Sewage-sludge biochar and iron-oxide-coated sands were tested to adsorb DNA and microorganisms carrying resistances.
- Up to 97% of genes tested were removed from the total environmental DNA of unfiltered effluent.
- Up to 85% of ARGs and MGEs of free-floating extracellular DNA were retained.
- Sewage-sludge biochar displayed the highest adsorption efficiencies.
- By-products from wastewater and drinking water treatment plants can be re-used for sanitation.

GRAPHICAL ABSTRACT
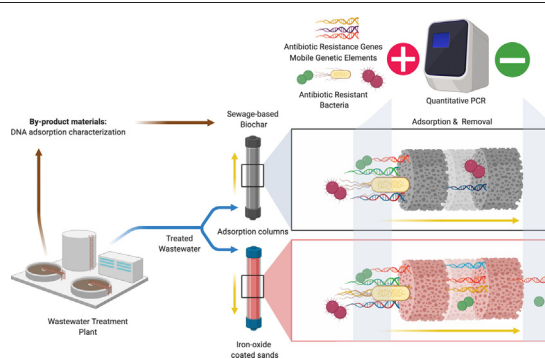
ARTICLE INFO

ABSTRACT

Wastewater treatment is challenged by the continuous emergence of chemical and biological contaminants. Disinfection, advanced oxidation, and activated carbon technologies are accessible in high-income countries to suppress them. Low-cost, easily implementable, and scalable solutions are needed for sanitation across regions. We studied the properties of low-cost absorbents recycled from drinking water and wastewater treatment plant residues to remove environmental DNA and xenogenetic elements from used water. Materials characteristics and DNA adsorption properties of used iron-oxide-coated sands and of sewage-sludge biochar obtained by pyrolysis of surplus activated sludge were examined in bench-scale batch and up-flow column systems. Adsorption

profiles followed Freundlich isotherms, suggesting a multilayer adsorption of nucleic acids on these materials. Sewage-sludge biochar exhibited high DNA adsorption capacity (1 mg g^{-1}) and long saturation breakthrough times compared to iron-oxide-coated sand (0.2 mg g^{-1}). Selected antibiotic resistance genes and mobile genetic elements present on the free-floating extracellular DNA fraction and on the total environmental DNA (*i.e.*, both extra/intracellular) were removed at 85% and 97% by sewage-sludge biochar and at 54% and 66% by iron-oxide-coated sand, respectively. Sewage-sludge biochar is attractive as low-cost adsorbent to minimize the spread of antimicrobial resistances to the aquatic environment while strengthening the role of sewage treatment plants as resource recovery factories.

1. Introduction

According to the UNICEF (2019), about 785 million people do not have access to potable water world-wide. Population growth and expanded living standards severely affect water resources availability (Shannon et al., 2008). New and alternate solutions to provide clean water are needed, such as wastewater reuse. The main problem with reclaiming wastewater is the final effluent quality. Sustainable Development Goals (SDG 6.3) targets high water quality by reducing the use of hazardous materials and increasing the proportion of treated water, thus stimulating recycling and safe reuse.

Wastewater treatment plants (WWTPs) are central to recycle used water to aquatic ecosystems. Located at the end of the sewer pipe, they face the full cocktail of pollutants emitted in the catchment area. WWTPs have been designed step-wise to remove pathogens, solids, organic matter, and nutrients like phosphorus and nitrogen. They are not designed to treat a number of persistent xenobiotic compounds, which are often discharged with the effluent (McEachran et al., 2018). Only a few countries have adopted water quality criteria to legislate the emissions and removal of micropollutants from wastewater, and their ecological impacts (Eggen et al., 2014; Weissbrodt et al., 2009). Both chemical and biological contaminants continuously emerge and rise concerns. New technical measures need to be developed to suppress xenobiotic compounds and xenogenetic elements.

Because of the microbial diversity of activated sludge, WWTPs are often hypothesized as hotspots for the horizontal gene transfer and proliferation of antimicrobial resistance (AMR) (Cacace et al., 2019; Rizzo et al., 2018). Rather than WWTPs *per se*, the whole set of emission sources in a catchment area needs to be considered at the root of AMR. The continuous release of antibiotics and other chemical and biological pollutants like heavy metals, antibiotic resistant bacteria (ARB), and antibiotic resistance genes (ARGs) in wastewater generates a selective pressure for AMR development and propagation in engineered and natural aquatic ecosystems. AMRs threaten the environmental, animal and human health, by the generation and spread of antibiotic-resistant pathogens across water bodies, soil, and food chain (Pruden et al., 2006; Tripathi and Tripathi, 2017). The overuse and misuse of antibiotics affect the medical effectiveness in combating pathogenic organisms (Lee Ventola, 2015; Gould et al., 2015).

In contrast to chemicals, AMRs are biological pollutants that replicate (Gillings et al., 2018). ARB are generated by horizontal transfer of ARGs and mobile genetic elements (MGEs) by and between microorganisms (Karkman et al., 2018). MGEs form the main component (65%) of extracellular DNA (exDNA) fragments that free-float in wastewater (Calderón-Franco et al., 2020a, 2020b). Stress conditions and complex microbial communities may enhance the transformation of microorganisms by these xenogenetic elements (Lu et al., 2015; von Wintersdorff et al., 2016).

A recent study of a set of six representative ARGs across more than 60 Dutch WWTPs has highlighted that WWTPs do not amplify the release of these intracellular ARGs (Pallares-Vega et al., 2019). ARGs and MGEs, such as the class I Integron-integrase gene (*intI1*), have been reduced on average of a 1.76 log unit from influents to effluents. However, 10^6 ARG copies are still present per liter of WWTP effluent. In a rough estimate, this corresponds to *ca.* 3–6·10^{14} ARG copies emitted per day or 1–2·10^{17} ARG copies emitted per year discharged in the outlet of large WWTPs of 1–4 million person-equivalents. The ARG content in the free-floating extracellular DNA fraction still remains unchecked and overlooked. Quantitative questions arise from water authorities on what level of ARGs can lead to a significant risk for environmental and human health. ARGs persist in river and lakes some kilometers away from the effluent discharge point (Czekalski et al., 2012). While the exposure of environmental, animal and human bodies to ARB and ARGs released from WWTP catchment areas into receiving waters has still to be addressed in order to address the risk, solutions to abate their loads are needed according to precautionary and/or prevention principles.

Tertiary treatments like effluent disinfection using UV or chlorination do not suppress the release of ARGs in the environment: these genes can still be detected in disinfected effluents (Pazda et al., 2019). Disinfection can inactivate or select for ARB (Destiani and Templeton, 2019; Wu and Xu, 2019; Yuan et al., 2015), while the genes can remain and can be released as free-floating exDNA by cell lysis. Most studies on the fate of AMRs (Yang et al., 2014) did not consider exDNA. The concentrations of free-floating exDNA measured from different wastewater samples (influent, activated sludge, and effluent) ranged between 2.6 and 12.5 μg L^{-1} (Calderón-Franco et al., 2020a). This exDNA fraction can persist several months or even years in marine and soil matrices (Mao et al., 2014; Torti et al., 2015). It can attach to suspended particles, sand, clay and humic acids (HAs). However, sorption of exDNA on natural particles does not prevent its mobility and ability to transform into natural competent bacteria (Zhang et al., 2018).

Different advanced technologies can remove ARB and ARGs from wastewater effluents. Process principles can go from solid-liquid separation in membrane bioreactors (Kappell et al., 2018; Riquelme Breazeal et al., 2013) to coagulation (Grehs et al., 2019; Li et al., 2017), disinfection and advanced oxidation *via* chlorination, ozonation, UV or UV-activated persulfate (Stange et al., 2019;(Zhou et al., 2020), besides algal-based wastewater treatment systems (Cheng et al., 2020) among others. The aforementioned physical-chemical methods however employ non-renewable materials or require consistent variations on the WWTP operation processes. These technological designs are mostly accessible in high-income countries. Simple, low-cost, implementable, and scalable solutions are needed for delivering safe sanitation worldwide according to local contexts.

In the water circular economy, upgrading resources recovered from the water cycle (Van Der Hoek et al., 2016) can be an efficient solution to remove AMR determinants. Sewage-sludge biochar produced by pyrolysis of surplus activated sludge is an interesting recycled resource for soil amendment to immobilize heavy metals (Cd, Cu, Ni, Pb or As) and prevent environmental risk of such chemicals (Agrafioti et al., 2013). Besides implementation of biochar soil, manure and solid waste management, implementation of sewage-sludge biochar for wastewater treatment is limited (Krzemiński and Popowska, 2020). Biochar from different sources has lately been studied for DNA and exDNA adsorption under different settings (Fang et al., 2021; Fu et al., 2021; Ngigi et al., 2020; Zhou et al., 2021). For instance, Fang et al. (2021) used local wood chip, wheat straw and peanut shell for biochar production to study adsorption and degradation by nucleases of extracellular DNA. Similar approach was followed by Fu et al. (2021), who used maize

straw to produce magnetic biochar to remove extracellular antibiotic resistance genes in aquatic environments. Zhou et al. (2021) and Ngigi et al. (2020) have proven that the addition of biochar from chicken manure and mushroom residues or pig manure does mitigate the accumulation and spread of ARGs during composting and storage.

Iron-oxide-coated sand are used to remove metals (As, Ni, and Zn) in drinking water treatment plants (WTP). Nucleic acids harbor phosphate-based polyanionic sites that can bind to iron or other multivalent cations. Therefore, DNA may exhibit ionic interactions with positively-charged materials like iron-oxide-coated sand (Vermeer et al., 1998; Vermeer and Koopal, 1998).

In a sanitation and circular economy approach, we studied the upgrading of by-products of wastewater and drinking WTPs as low-cost adsorbents to remove environmental and free-floating exDNA. Sewage-sludge biochar prepared by pyrolysis of dewatered sewage sludge and used iron-oxide-coated sands were reclaimed for their adsorption characteristics and capacity to remove ARGs and MGEs as well as ARB from secondary wastewater effluents. We characterized the adsorbents by X-ray fluorescence spectrophotometry, Mössbauer spectroscopy, and scanning electron microscopy. We measured the DNA adsorption isotherms of the adsorbents and breakthrough curves of both free-floating exDNA and total environmental DNA (*i.e.*, microorganisms and exDNA) from batch to up-flow fixed-bed column systems. Our results help delineate the potential of these cheap recycled materials to prevent the release of ARB, ARGs and MGEs in WWTP effluents into aquatic ecosystems.

2. Material and methods

2.1. Preparation of sewage-sludge biochar by pyrolysis of dewatered activated sludge and collection of iron-oxide-coated sand

Dewatered sewage sludge was collected from the urban WWTP Harnaschpolder (Waterboard Delfland, The Netherlands) to produce sewage-sludge biochar. The dewatered sewage sludge samples were brought to the lab within 1 h and stored at 4 °C pending analyses and pyrolysis. Before pyrolysis, the sewage sludge was characterized by moisture content and volatile matter. The moisture content was performed at 11 ± 1 °C and volatile matter at 500 ± 50 °C until constant weight was achieved. Sewage-sludge biochar was produced following Agrafioti et al. (2013). Dewatered sludge was heated in a muffle furnace at 600 °C under a controlled flow of nitrogen. The temperature increase rate was kept at 17 °C min^{-1}. The samples were kept for 30 min residence time. Oxygen-free conditions were maintained by supplying nitrogen at a rate of 200 mL min^{-1}. The cooled samples were then crushed and sieved at 150 μm pore size. Biochar generation by pyrolysis was done in triplicates at one selected temperature (600 °C). The methodology for analyzing the properties of the raw material used for the production of biochar was followed according to Agrafioti et al. (2013). The sewage-sludge biochar production yield was determined as the ratio of the produced dry mass of sewage-sludge biochar (after pyrolysis) to the dry mass of sewage-sludge (before pyrolysis). The sewage-sludge biochar was stored at room temperature pending experiments.

An amount of 2 kg of used iron-oxide-coated sand (1–4 mm) was reclaimed from the sand-filtration unit of AquaMinerals B.V., a water sanitation company giving a second life to the resources from drinking WTPs in The Netherlands. Iron-oxide-coated sands received were crushed and sieved at 600 μm, and stored at room temperature for further experiments.

Other sorbents were tested as comparison basis, namely powdered activated carbon (PAC), granular activated carbon (GAC), and mineral wool.

2.2. Sampling of effluent water from WWTP

Effluent water was collected from WWTP Harnaschpolder operated for full biological nutrient removal. Effluent water was collected at the outlet of its tertiary treatment. Sample triplicates were collected on

three different days. A volume of 1 L of treated water was collected per replicate. All samples were processed in a timeframe of less than 4 h after collection.

2.3. Physical-chemical analyses of the adsorbents

2.3.1. Chemical compositions of the adsorbents

The inorganic chemical composition of sewage-sludge biochar was characterized using an Axios Max wavelength dispersive X-ray fluorescence (WD-XRF) spectrophotometer (Malvern-Panalytical, The Netherlands). The data was evaluated with SuperQ5.0i/Omnian software. Carbon (C), oxygen (O) and nitrogen (N) could not be measured by WD-XRF spectrophotometry. The elemental composition of carbon (C), oxygen (O), hydrogen (H), nitrogen (N) and sulphur (S) from sewage-sludge biochar and of iron (Fe) and silica (Si) from iron-oxide-coated sand were analyzed by elemental analysis (Mikrolab Kolbe, Germany).

2.3.2. Surface area and pore size of the adsorbents

The surface area and pore size of the adsorbents were calculated using a nitrogen gas adsorption analyser (Micrometrics Gemini VII 2390 Surface area analyser, USA). Before analysis, 5 g of the by-product materials were previously degassed under vacuum at 150 °C (under N_2 flow) during 1 h to eliminate moisture and gasses. A mass of 0.5 g of the by-product materials was introduced in the test tube with liquid nitrogen. N_2 isotherms were measured at -196 °C. Surface area was calculated according to the Brunauer-Emmett-Teller (BET) method (Naderi, 2015), which incorporates a multilayer coverage. The Barret-Joyner-Halenda (BJH) method was used to determine the pore size using Kelvin equation of pore filling, where a cylindrical pore geometry was assumed (Villarroel-Rocha et al., 2014).

2.3.3. Valence state of iron-oxide-coated sands

The valence state of iron (Fe) in iron-oxide-coated sand was determined by Mössbauer Spectroscopy to retrieve its oxidation state. Mössbauer spectra were recorded at 300 K with a conventional constant-acceleration spectrometer, and at 4.2 K (liquid helium cryostat) with a sinusoidal velocity spectrometer, using a ^{57}Co (Rh) source. A velocity calibration curve was performed using an α-Fe foil at room temperature.

2.3.4. Surface observation of adsorbents by scanning electron microscopy

The surface observation of sewage-sludge biochar and iron-oxide-coated sand was analyzed using a scanning electron microscope (SEM; model JSM-6010LA, Jeol Ltd., Japan) at magnifications of 5'000-10'000× and acceleration voltages of 5–15 keV.

2.4. DNA standard solutions and chemicals used for adsorption experiments

Solutions of UltraPure™ Salmon sperm DNA (Thermo Fisher Scientific, USA) were used as standards for free-floating exDNA in order to characterize DNA adsorption phenomena in batch and column regimes, before testing the removal of total environmental DNA from WWTP effluent. Salmon sperm DNA is double stranded, and sheared to an average size of ≤2000 bp. The purity of DNA was assessed by UV light absorbance at 260 and 280 nm ($A_{260/280} > 1.8$) (BioTek, Gen5 plate reader, USA).

The chemicals and other reagents were obtained from Sigma Aldrich (USA). In order to assess the effect of different ions and humic acids on DNA adsorption, stock solutions of 1 mol L^{-1} of salts (NaCl, CaCl$_2$.2H$_2$O, MgCl$_2$.6H$_2$O) and 800 mg L^{-1} of humic acids (CAS No. 1415-93-6) were prepared in ultrapure water (Sigma Aldrich, UK).

2.5. DNA adsorption in batches

2.5.1. Preliminary screening of adsorbents

The adsorption efficacies of sewage-sludge biochar and iron-oxide-coated sand were compared to those of powdered activated carbon

(PAC), granular activated carbon (GAC), and mineral wool as reference materials. Adsorption efficacies were preliminarily tested in triplicate experiments conducted in 2-mL sterile Eppendorf tubes with 40 mg of tested adsorbent material and 1 mL of working solutions of salmon sperm DNA at initial concentrations of 0, 20, 40, 60, 80, 100, 120 and 140 µg DNA mL^{-1} in either ultrapure water, tap water, and filtered (0.2 µm) WWTP effluent water. The Eppendorf tubes were mixed continuously at 180 rpm on an orbital shaker at 25 °C until equilibrium. The mixture was then centrifuged at 13000 ×g for 20 min prior to measuring the DNA concentration from the supernatant (BioTek, Gen5 plate reader, USA).

2.5.2. DNA adsorption equilibria of sewage-based biochar and iron-oxide-coated sand

To find the equilibrium time required for DNA adsorption onto sewage-based biochar and iron-oxide-coated sand, batch experiments were conducted in apothecary glass bottles of 25 mL, with a working solution of 5 mL of salmon sperm DNA at an initial concentrations of 100 µg DNA mL^{-1} in ultrapure water, tap water, and filtered effluent water. The mass of sewage-sludge biochar or iron-oxide-coated sand adsorbents was added in increasing amounts from 0 to 100 mg adsorbent mL^{-1} in separate bottles. Each experiment was performed in triplicates. The bottles were agitated continuously at 180 rpm on an orbital shaker at 25 °C for 24 h. Liquid volumes of 0.5 mL were sampled every 1 h from the batches and centrifuged at 13000 ×g for 20 min.

2.5.3. Effect of pH, ionic strength and humic acids content on DNA adsorption

To evaluate the influence of pH on DNA adsorption, experiments were run at pH 5, 7 and 9 in 10 mmol L^{-1} Tris-HCl buffer with initial DNA concentrations of 20 and 100 µg DNA mL^{-1}. The interaction effects of cation species on DNA adsorption was studied at initial DNA concentration of 100 µg DNA mL^{-1} in the presence of 0–60 mmol L^{-1} Na$^+$ (as NaCl), Mg^{2+} (as MgCl$_2$), and Ca^{2+} (as CaCl$_2$) at pH 7. Competition with organic matter on DNA adsorption was investigated at pH 7 in the presence of humic acids (HAs) at 0–100 mg HAs L^{-1} to represent natural organic matter. In all experiments, pH was maintained constant in Tris-HCl buffer.

2.5.4. Quantifying the DNA adsorbed on sewage-sludge biochar and iron-oxide-coated sand

The residual DNA concentration in the supernatants was measured in 96-well UV flat-bottom plates (Greiner UV Star 96, Germany) by UV spectrophotometry at 260 nm (BioTek, Gen5 plate reader, USA). The DNA concentration after incubation with HAs was measured with Qubit® dsDNA assays (Thermo Fisher Scientific, USA) (Leite et al., 2014). The amount of DNA adsorbed onto the adsorbent at equilibrium was calculated using Eq. (1).

$$Amount\ of\ DNA\ adsorbed\ \left(\frac{µg\ DNA}{mg\ adsorbent}\right)$$

$$= \frac{[DNA]_0\left(\frac{µg}{mL\ water}\right) - [DNA]_{final}\left(\frac{µg}{mL\ water}\right)}{Adsorbent\ weight\ (mg)} \times Sample\ volume\ (mL) \tag{1}$$

2.5.5. Modelling DNA adsorption isotherms and efficiency

Both Langmuir and Freundlich isotherm models were applied to describe the DNA adsorption from the solution onto the adsorbents.

The Langmuir isotherm model (Eq. (2)) describes the adsorption of adsorbate molecules (DNA in this case) by assuming behavior as an ideal gas under isothermal conditions. Adsorption is supposed to happen onto homogeneous solid surfaces that exhibit one adsorption site.

$$q_e = \frac{q_{max}K_L C_e}{1 + K_L C_e} \tag{2}$$

where q$_e$ (mg adsorbate g^{-1} adsorbent) is the amount of adsorbate adsorbed, C$_e$ (mg adsorbate L^{-1}) is the equilibrium adsorbate concentration, q$_{max}$ (mg adsorbate g^{-1} adsorbent) is the maximum monolayer adsorption capacity, and K$_L$ (L mg^{-1} adsorbate) is the Langmuir empirical constant related to the heat of adsorption. K$_L$ represents the adsorption affinity of the adsorbate onto the adsorbent.

The Freundlich isotherm model (Eq. (3)) is an empirical relation between the concentration of a solute on the surface of an adsorbent (by-products) and the concentration of the solute in the liquid at its interface. The Langmuir model assumes only a monomolecular layer on the surface at maximum coverage (*i.e.*, no stacking of adsorbed molecules). The Freundlich isotherm does not account for this restriction.

$$q_e = K_F C_e^{1/n} \tag{3}$$

where q$_e$ (mg adsorbate g^{-1} adsorbent) is the amount of solute adsorbed, C$_e$ (mg adsorbate L^{-1}) is the equilibrium adsorbate concentration, K$_F$ (mg adsorbate g^{-1} adsorbent) is the Freundlich constant related to the adsorption capacity, and n (−) is the heterogeneity factor and adsorption favorability.

2.6. DNA adsorption in up-flow packed-bed column

2.6.1. Characteristics of the columns packed with sewage-sludge biochar and iron-oxide-coated sand

Continuous up-flow adsorption experiments were conducted in chromatography glass columns (1 cm inner diameter and 15 cm column). An amount of 0.5 g of glass beads (250–300 µm) was inserted at the bottom of the column for a homogeneous flow distribution through the column. The columns were packed with known quantities of adsorbents: 3 g of sewage-sludge biochar and 4 g of iron-oxide-coated sand.

2.6.2. Hydraulic residence time in the packed column

Hydraulic residence time distributions in the up-flow columns packed with either sewage-sludge biochar or iron-oxide-coated sand were recorded using a NaCl salt tracer (Fig. S2 in Supplementary material). The columns were filled with the sorbents at a bed height of 10 cm and fed with a saline solution at a flow rate of 1 mL min^{-1}. A concentration of 60 mmol L^{-1} NaCl salt solution (*i.e.*, 3.5 g L^{-1}) was pulse-dosed at the column foot by using an HPLC liquid chromatography pump (Shimadzu LC-8A, USA). The concentration changes in the effluent were measured by electrical conductivity using a PRIMO 5 Microprocessor Conductivity Meter (Hanna instruments, USA), as a function of time by taking liquid samples of 0.5 mL from the column outlet.

2.6.3. Breakthrough of salmon sperm DNA in the up-flow packed column

The packed columns were fed up-flow with aqueous standard solutions of salmon sperm DNA of known concentrations using an HPLC liquid chromatography pump (Shimadzu LC-8A, USA). Adsorption breakthrough curves were recorded (*i*) with inlet DNA concentrations of 0.1, 0.3 and 0.5 mg DNA L^{-1} at a fixed flow rate of 0.1 mL min^{-1} and (*ii*) with flow rates of 0.1, 0.3 and 0.5 mL min^{-1} at a fixed inlet DNA concentration of 0.3 mg DNA L^{-1}. Samples of 200 µL were collected at the column outlet in intervals of 15 min. The DNA concentration was measured spectrophotometrically until the ratio of C$_t$/C$_o$ reached a constant value: C$_o$ and C$_t$ are the DNA concentrations at the column inlet and outlet, respectively. A Ct/C$_o$ ratio close to 1 indicates saturation of the column with DNA (*i.e.*, full adsorption capacity reached).

2.6.4. Data analysis of DNA breakthrough curves and maximum adsorption capacities in column

The performance of a fixed bed column can be explained by the breakthrough curves. The amount of time needed for breakthrough and the shape of the curve inform on the dynamic behavior of the column. Breakthrough curves are expressed as C_t/C_o versus time (Han et al., 2009; Rouf and Nagapadma, 2015). The breakthrough point is usually defined as the point when the ratio between influent concentration, C_0 (mg L^{-1}) and outlet concentration, C_t (mg L^{-1}) becomes 0.05 to 0.90 (Chowdhury et al., 2015). The total capacity of the column (q_{total} in mg) gives the maximum amount of DNA that can be adsorbed and is calculated by integrating the area under the breakthrough curve given by Eq. (4) (Chen et al., 2012; Han et al., 2009; Rouf and Nagapadma, 2015)

$$q_{total} = \frac{Q}{1000} \int_{t=0}^{t=total} C_{ad} \, dt \tag{4}$$

where Q is the flow rate (mL min^{-1}); "t = total" is the total flow time (min); C_{ad} is the adsorbed DNA concentration ($C_o - C_t$) (mg L^{-1}).

The equilibrium DNA uptake or maximum adsorption capacity of the column $q_{eq(exp)}$ (mg g^{-1}) is calculated by Eq. (5):

$$q_{eq(\ exp)} = \frac{q_{total}}{m} \tag{5}$$

where m is the dry weight of the adsorbent in the column (g).

2.6.5. Modelling DNA adsorption in the fixed-bed column

The column data were fitted with Thomas and Yoon-Nelson models for column modelling as in Chatterjee et al. (2018). In order to design an adsorption column, predicting the breakthrough curve and adsorbent capacity for the adsorbate under certain conditions is required. Data obtained from the experiments can be used for designing a prospective full-scale column operation.

The Thomas model (Eq. 6) was used to estimate the absorptive capacity of the adsorbent in the column.

$$\frac{C_t}{C_o} = \frac{1}{1 + exp\left[\left(\frac{K_{TH} \, q_e \, x}{Q}\right) - k_{Th} \, C_o \, t\right]} \tag{6}$$

where k_{TH} (mL min^{-1} mg^{-1}) is the Thomas model constant; q_e (mg g^{-1}) is the predicted adsorption capacity; x is the mass of adsorbent (g); Q is the flow rate (mL min^{-1}); C_o is the inlet DNA concentration (mg L^{-1}); C_t is the outlet DNA concentration at time t (mg L^{-1}).

The Yoon-Nelson model (Eq. 7) was used to predict the run time before regeneration or replacement of the column becomes necessary. It is a very simple model to represent the breakthrough curve: it does not require any data about the characteristics of the system and the physical properties of the adsorbent (Rouf and Nagapadma, 2015).

$$\frac{C_t}{C_o - C_t} = \ exp(K_{YN}t - \tau k_{YN}) \tag{7}$$

where K_{YN} (min^{-1}) is the rate constant; τ (min) is the time required for 50% adsorbate breakthrough.

2.7. Removal of ARGs and ARB from filtered and unfiltered WWTP effluents in up-flow columns

After the detailed characterization of DNA adsorption properties with synthetic solutions of salmon sperm DNA, the column experiments were performed by feeding a real effluent water from WWTP Harnashpolder to the packed columns.

2.7.1. Experiments with filtered and unfiltered real WWTP effluent

Two sets of experiments were run with filtered (0.2 μm) and unfiltered WWTP effluent water to characterize the removal of free-floating exDNA and of total environmental DNA (i.e., both intracellular and extracellular DNA), respectively, and their related ARG/MGE content. The experiments were performed in triplicates. Volumes of 1 L of filtered/unfiltered WWTP effluent were passed through the columns at up-flow feeding flowrate of 0.3 mL min^{-1}. The removals of ARGs and ARB were measured by comparing their levels in the free-floating exDNA fraction and total environmental DNA of the inlet and outlet of the packed column. The extractions and purification procedures of free-floating exDNA and total environmental were described in details elsewhere (Calderón-Franco et al., 2020b) and given in short hereafter.

2.7.2. Isolation of free-floating extracellular DNA from WWTP effluent matrices

To extract the free-floating exDNA, sample volumes of 1 L were filtered sequentially through 0.44 μm and 0.22 μm polyvinylidene fluoride (PVDF) membranes (Pall Corporation, USA) prior to isolation by ion exchange. The DEAE ion-exchange column was prepared and processed according to manufacturer's instructions. Buffers and solutions used for equilibrating, eluting, regenerating, cleaning and storing the DEAE ion-exchange column are the following. The equilibration buffer consisted of 50 mmol L^{-1} Tris, 10 mmol L^{-1} EDTA at pH 7.2. The elution buffer consisted of 50 mmol L^{-1} Tris, 10 mmol L^{-1} EDTA, 1.5 mol L^{-1} NaCl at pH 7.2. The regeneration buffer consisted of 50 mmol L^{-1} Tris, 10 mmol L^{-1} EDTA, 2 mol L^{-1} NaCl, pH 7.2. The cleaning solution consisted of 1 mol L^{-1} NaOH and 2 mol L^{-1} NaCl. The storage solution consisted of 20% ethanol in ultrapure water.

The full volume (1 L) of the pre-filtered sample containing the free-floating exDNA was loaded in a positively charged 1-mL diethylaminoethyl cellulose (DEAE) ion-exchange column (BIA Separations, Slovenia) at a speed of 0.6 mL min^{-1} after equilibration in order to keep the pressure below the maximum limit of 1.8 MPa. After chromatographic retention, the exDNA was eluted at a flowrate of 1 mL min^{-1} with elution buffer and tracked over time with an HPLC photodiode array detector (Waters Corporation, USA) recording the UV-VIS absorption of DNA at 260 nm.
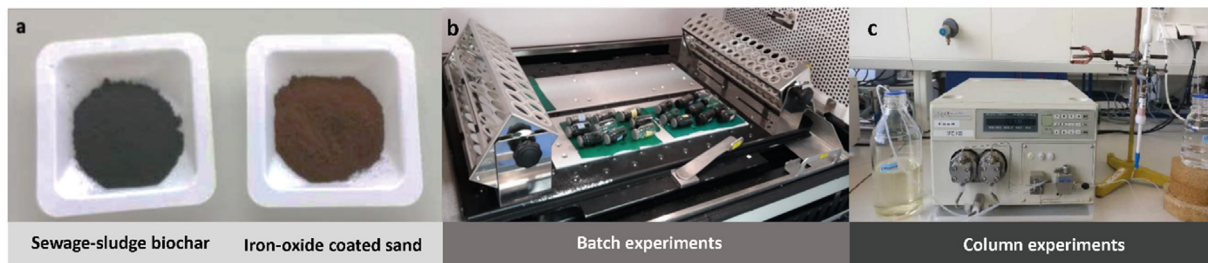
Fig. 1. From waste by-products to DNA adsorbents at the root of circular water economy. (a) Macroscopic visualization of sewage-sludge biochar prepared by pyrolysis at 600°C of dewatered surplus activated sludge from a wastewater treatment plant and of used iron-oxide-coated sand reclaimed from a drinking water treatment plant. Batch (b) and continuous-flow column (c) setups used to characterize the DNA adsorption isotherms, characteristics, and efficiencies of the two reclaimed adsorbent materials.

The recovered raw free-floating exDNA was precipitated from the eluate with ethanol (Moore and Dowhan, 2002). The residual proteins bound to the exDNA were digested by 2-h incubation with 0.85 g L^{-1} proteinase K (Sigma-Aldrich, UK); the enzymatic reaction was stopped at 50 °C for 10 min. The protein-digested raw free-floating exDNA sample was finally purified using GeneJET NGS Cleanup Kit (Thermo Scientific, USA). The purified free-floating exDNA isolates were stored at −20 °C pending analysis.

2.7.3. Extraction of total environmental DNA from WWTP effluent matrices

The total environmental DNA (*i.e.*, intracellular and extracellular DNA) was extracted from the unfiltered water sample before loading the column and the effluent using the DNeasy Power Water kit (Qiagen, The Netherlands) following manufacturer's instructions. All DNA extracts were quantified by fluorometry using Qubit® (Thermo Fisher Scientific, USA).

2.8. Quantification of ARGs and MGE by quantitative polymerase chain reaction

The 16S rRNA gene was selected as a proxy to quantify total bacteria. The genes analyzed by qPCR (Table 1) were chosen from a selection panel of ARGs previously used for wastewater survey (Pallares-Vega et al., 2019). These ARGs confer resistance to antibiotics with the highest consumption in The Netherlands: erythromycin macrolides (*ermB*), sulfonamides (*sul1* and *sul2*), quinolones (*qnrS*) and extended-spectrum β-lactamase (*bla$_{CTX-M}$*). The class 1 integron-integrase gene (*intI1*) – a jumping gene driving horizontal gene transfer (Ma et al., 2017) – was included to assess the fate of MGEs. Standards for qPCR were generated from a curated antimicrobial resistance genes database ResFinder (https://cge.cbs.dtu.dk/services/ResFinder/). Standards, primers, and reaction conditions are listed in Tables S1 and S2 in Supplementary material.

3. Results and discussion

The preliminary screening of adsorbents revealed the interesting DNA adsorption characteristics of sewage-sludge biochar close to powdered activated carbon (Fig. 3). Depending on concentrations of salmon sperm DNA standard and its ratio to adsorbent mass (20–140 μg DNA mL^{-1} for 40 mg of adsorbent material in 1 mL working volumes in Eppendorf tubes), and on water conditions from ultrapure water to tap water to filtered WWTP effluent, the sewage-sludge biochar and used iron-oxide-coated sand displayed superior adsorption potential than granular activated carbon and mineral wool. Powdered activated carbon is industrially manufactured and forms a definite solution to remove potentially problematic environmental DNA on top of chemical micropollutants. Sewage-sludge biochar and used iron-oxide coated sand are reclaimed from WWTP and drinking WTP wastes, rendering these adsorbents as interesting low-cost mitigation solutions in the context of the circular water economy. A detailed examination of the physical-chemical properties of DNA adsorption onto these two circular products is elaborated in this study (Fig. 2).

3.1. Physical-chemical characteristics of sewage-sludge biochar and iron-oxide-coated sand are suited for DNA adsorption and microbial retention

The surface morphologies of the sewage-sludge biochar processed by pyrolysis (600 °C) of surplus activated sludge from the WWTP (Fig. 4a-b) and of reclaimed iron-oxide-coated sand obtained from the drinking WTP (Fig. 4c-d) were characterized by SEM. The surface morphologies of both by-products were highly heterogeneous and structurally complex, with many pores of different diameters. No fibers nor debris structures were observed in any of the materials.

The specific surface areas measured according to Brunauer-Emmett-Teller (BET) are provided in Table 2. The surface area of sewage-sludge biochar (32.4 m^2 g^{-1}) was lower than iron-oxide-coated sand (164.9 m^{2}g^{-1}). Ash filling, which blocks access to the biochar micropores, could explain this difference (Song and Guo, 2012). Méndez et al. (2013) got similar BET surface area values (37.18 m^2 g^{-1}) and pore diameter (9.46 nm) for sewage-sludge biochar pyrolyzed at same temperature.

Sharma (2001) described the specific surface area of iron-oxide-coated sand from 12 different Dutch drinking WTP in the range of 5.4 to 201 m^2 g^{-1}. They suggested that the BET surface area of iron-oxide-coated sand could mainly depend on their residence time (from months to years) in the drinking WTP.

The relatively low yield of sewage-sludge biochar production of 0.39 g dried sewage-sludge biochar g^{-1} dried sewage sludge matches other studies (Roberts et al., 2017; Tarelho et al., 2019). The biochar production yield has a direct implication on its industrial applicability. It highly varies on the pyrolysis temperature used (Daful and Chandraratne, 2018) since directly linked to amounts of volatile matter released (Titiladunayo et al., 2012). For practice, other pyrolysis temperatures and seasonal biomass samples could be tested to address variations in the biochar production yield and its DNA adsorption capacity. Biochar-based systems form an important low-cost component to sustain sanitation in low- and middle-income countries. Sunlight-based processes are currently investigated to concentrate energy in solar furnaces to drive photothermal processes across a temperature range from 80 to more than 1000 °C, thus perfectly suited for biochar production (Ayala-Cortés et al., 2019) from any kind of biomasses locally available.

The chemical properties of the adsorbent materials are presented in Table 2. The sewage-sludge biochar was mainly composed of oxygen, sulphur and carbon with traces of other elements like phosphorus, magnesium or calcium bioaccumulated during wastewater treatment. Iron-oxide-coated sands mainly comprised iron, oxygen and silica. The valence state of iron in the iron-oxide-coated sand was determined by Mössbauer spectroscopy, resulting in mainly ferrihydrite (III) particles (Fig. S1; Table S3).

The porous morphologies and chemical characteristics of sewage-based biochar and iron-oxide-coated sand exhibit interesting properties for exDNA removal by entrapment and adsorption.

3.2. Adsorption of nucleic acids by sewage-sludge biochar and iron-oxide-coated sand is governed by a multilayer Freundlich isotherm

From the batch tests performed in apothecary glass bottles of 25 mL with 5 mL working volumes, initial salmon sperm DNA concentrations of 100 μg DNA mL^{-1} and increasing amounts of adsorbents from 0 to 100 mg mL^{-1}, sewage-sludge biochar rapidly and efficiently removed the DNA present in the supernatant after 2 h equilibrium time onto 40–100 mg adsorbent mL^{-1} (Fig. 5a-b). Reclaimed iron-oxide-coated sand displayed lower DNA adsorption capacity with a minimum of 80 mg adsorbent mL^{-1} needed to fully remove the DNA after an equilibrium time of at least 5 h. One may raise the question on whether the

Table 1
Details of the panel of universal 16S rRNA gene, antibiotic resistant genes (ARGs), and mobile genetic element (MGE). The selection was based on Pallares-Vega et al. (2019) as representative genes for The Netherlands.

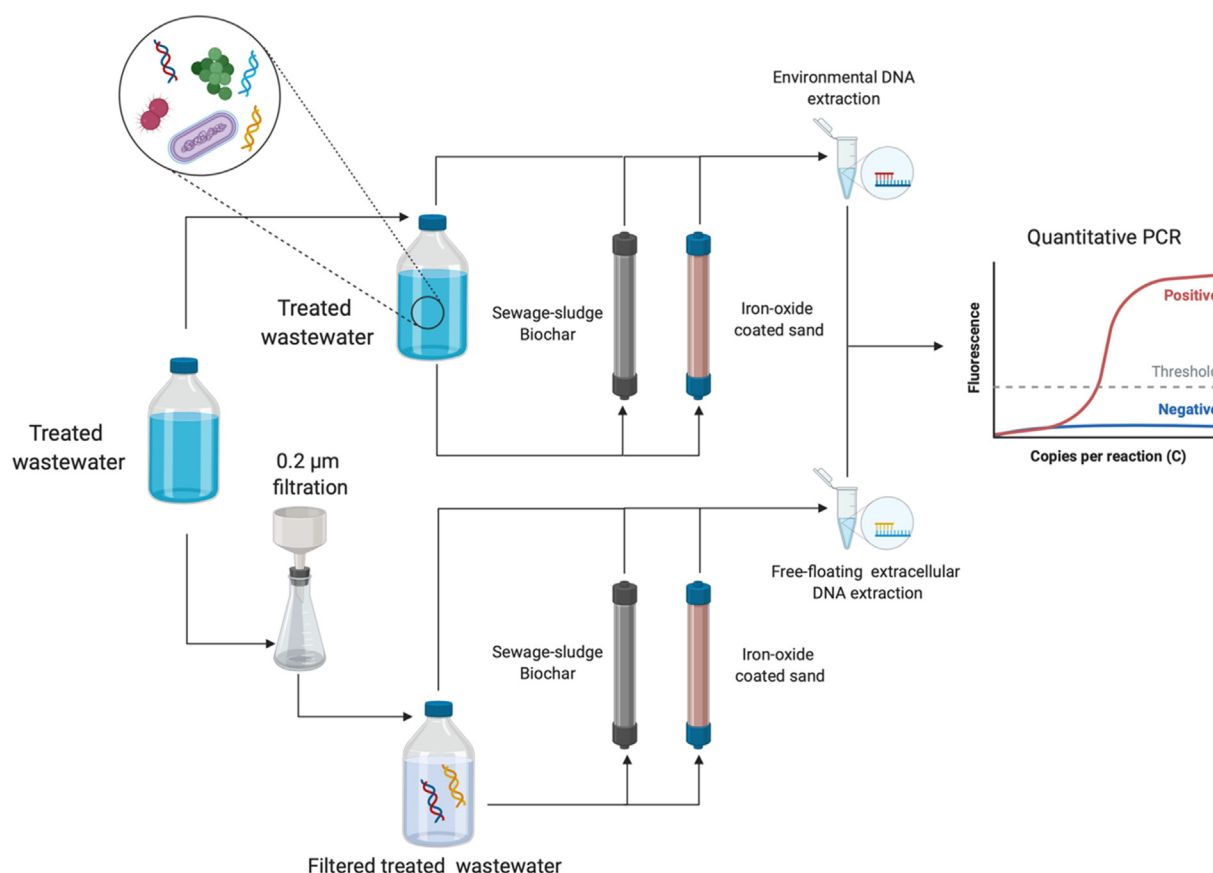| Group	Gene	Function
All Bacteria	*16S ribosomal RNA gene*	Normalization to the concentration of bacteria
ARGs	*ermB (Erythromycin resistance)*	Resistance to macrolides
	sul1 (Sulfonamide resistant dihydropteroate synthase 1)	Resistance to sulfonamides
	sul2 (Sulfonamide resistant dihydropteroate synthase 2)	Resistance to sulphonamides
	qnrS (Fluoroquinolone resistance)	Resistance to quinolones
	bla$_{CTXM}$ (Cefotaxime-hydrolyzing β-lactamase resistance)	Resistance to extended spectrum β-lactams
MGE	*intI1 (Class 1 Integrase)*	Integrase of type 1 integrons

Fig. 2. Schematic representation of the experimental adsorption column setup used and the quantitative PCR as analytical procedure applied. The aim was to study the adsorption and removal of antibiotic resistance bacteria, antibiotic resistance genes and mobile genetic elements by using sewage- sludge biochar and iron oxide-coated sand from treated effluent wastewater. Detail of material and setup used can be found in Fig. 1. Created with *BioRender*.

DNA removal occurred *via* adsorption or degradation. DNA did not show any degradation after 24 h of suspension in treated wastewater without any sewage-sludge biochar (Fig. 5a). Recent studies have shown that the presence of biochar provided protection to exDNA against degradation by DNase I (Fang et al., 2021). In addition, cross-verification methods like DNA fluorescence staining and microscopy could be used to consolidate adsorption results.

Both Langmuir and Freundlich isotherm models were used to analyze the DNA adsorption patterns on the two adsorbents (Fig. 5c-d, Table 3). The Freundlich isotherm model was better describing the DNA adsorption profiles ($R^2 = 0.99$ and 0.93 for sewage-sludge biochar and iron-oxide-coated sand, respectively, on filtered WWTP effluent water) than the Langmuir monolayer isotherm model ($R^2 = 0.92$ and 0.89, respectively). This suggested a multilayer adsorption of DNA with heterogeneous distribution of active adsorption sites, agreeing with already published literature (Fang et al., 2021).

Table 3 compares the calibrated parameters of both adsorption models onto both adsorbent materials in ultrapure water and in filtered WWTP effluent water. Sewage-sludge biochar revealed a higher Freundlich constant K_F (1 mg DNA g^{-1} adsorbent on effluent water) than iron-oxide-coated sand (0.21 mg DNA g^{-1} adsorbent). For a thermodynamically favorable adsorption, the exponent constant n for a given adsorbate and adsorbent at a particular temperature should lie between 1 and 10 (Desta, 2013). This was the case for both adsorbents.

Sewage-sludge biochar was a more effective DNA adsorbent with higher affinity towards nucleic acids than iron-oxide-coated sand. It is important to highlight that the binding mechanisms differ between the two types of materials: hydrophobic forces rule adsorption on sewage-sludge biochar while the phosphate groups of DNA binds to iron of the iron-oxide-coated sand.

3.3. No effect of pH and coexisting anions was observed on DNA adsorptions

The influence of pH on DNA adsorption was analyzed in Tris-HCl buffer medium at initial salmon sperm DNA concentrations of 20 and 100 mg DNA L^{-1} (Fig. 6a-b), but not significant effect of pH was observed on DNA adsorption capacity onto the tested materials.

Organic clays, montmorillonite and biochar can adsorb more DNA under acidic (pH < 5) than alkaline (pH > 9) conditions (Cai et al., 2006c; Saeki and Kunito, 2010). Biochar surfaces display an increased negative charge from pH 3 to 7 (Yuan et al., 2011). The isoelectric point of DNA is about pH 5 (Cai et al., 2006b). Phosphate groups confer a negative charge to DNA macromolecules when pH is above the isoelectric point. At low pH < 2, DNA mostly presents neutral electrical properties. In order to avoid electrostatic repulsion, sewage-sludge biochar and DNA should not be negatively charged simultaneously. At pH below 4, both biochar surfaces and DNA phosphate groups are protonated, decreasing repulsion between them and increasing the DNA adsorption capacity. However, these theoretical principles do not align with our experimental results. Wang et al. (2014) have similarly observed that pH shifts did not impact the adsorption of nucleic acids on willow-wood biochar. We conclude that DNA is mostly adsorbed *via* hydrophobic interactions rather than electrostatic ones.

Adsorption of ortho-phosphate onto iron-oxide-coated sand increase as the pH decreases, following an anionic adsorption behavior (Huang et al., 2014). In our case, pH shifts did not show any significant effect on DNA adsorption by the phosphate groups.

Fig. 6c presents the influence of ionic conditions on salmon sperm DNA adsorption at pH 7, initial concentration of 100 mg DNA L^{-1}. Na^+ and Ca^{2+} addition at 1–60 mmol ion L^{-1} had no significant effect ($p > 0.05$) on DNA adsorption onto sewage-sludge biochar and
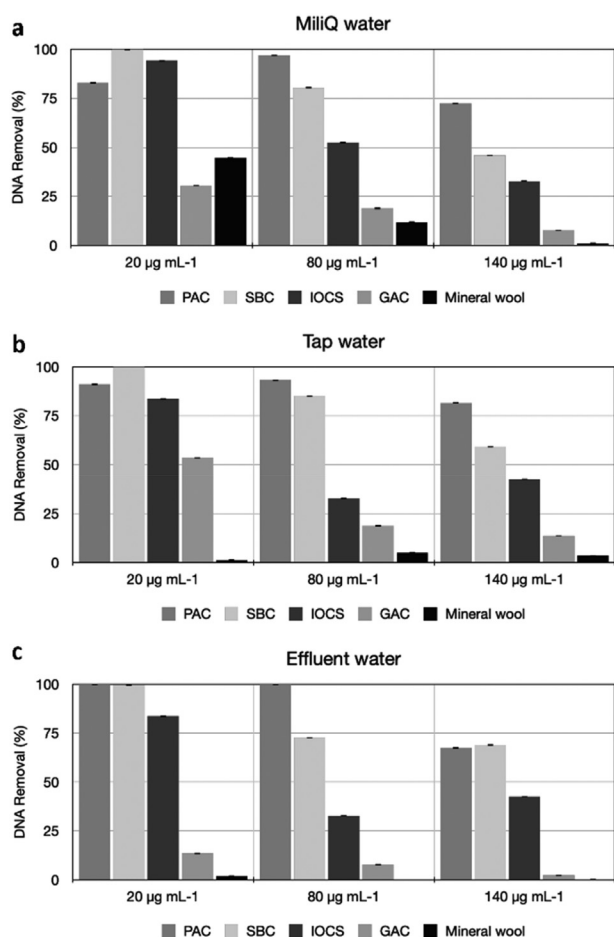
Fig. 3. Removal of salmon sperm DNA standard by powdered activated carbon (PAC), sewage-based biochar (SBC), iron oxide coated sands (IOCS), granular activated carbon (GAC) and mineral wool in (a) ultrapure water, (b) tap water, and (c) effluent wastewater.

iron-oxide-coated sand (Supplementary Table S4). Only the addition of 60 mmol Mg^{2+} L^{-1} in the test with sewage-sludge biochar displayed a significant increase of 33% ($p < 0.05$) in DNA adsorption capacity (0.89 mg DNA g^{-1} adsorbent).

Ion bridges and charge neutralization are the supposed main mechanisms increasing DNA adsorption by cations addition (Cai et al., 2006a; Nguyen and Chen, 2007). However, DNA adsorption onto these materials did not seem to be driven by electrostatic interactions. For this reason, it is hypothesized that hydrophobic interactions or iron-phosphate interactions can play a role in the DNA adsorption onto the sewage-sludge biochar and iron-oxide-coated sand, respectively. Higher pyrolysis temperatures (>600 °C) significantly increase the DNA adsorption efficiency by enhancing the surface area and hydrophobicity of the biochar (Dai et al., 2017).

3.4. Sewage-sludge biochar is an efficient adsorbent for DNA removal in up-flow column systems

Two bench up-flow 15 × 1 cm chromatography glass columns equipped with 0.5 g of glass beads (250–300 μm) surmounted by 3 g of sewage-sludge biochar or 4 g of iron-oxide-coated sand particles filling were evaluated for the continuous-flow adsorption of salmon sperm DNA standard out of ultrapure water and of filtered WWTP effluent water.

The hydraulic residence time distributions (RTDs) measured by spiking NaCl at 60 mmol L^{-1} in the water flow displayed plug-flow patterns with axial dispersion in these column systems (Fig. S2 in Supplementary information). Iron-oxide-coated sand displayed a sharper peak but with long tailing. The RTD with sewage-sludge biochar was more equilibrated with a Gaussian shape. Both RTDs harbored a peak maximum (mode) at 10 min at a flow-rate of 1 mL min^{-1}.

The DNA breakthrough curves are depicted in Fig. 7. In agreement with batch results, sewage-sludge biochar was more effectively adsorbing DNA than iron-oxide-coated sand from these water matrices. In ultrapure water, the effect of the adsorbent material on the breakthrough point was remarkable, *i.e.*,10.4 ± 1.9 times (depending on initial DNA concentrations of 0.1–0.5 mg DNA mL^{-1}) and 4.3 ± 0.9 times
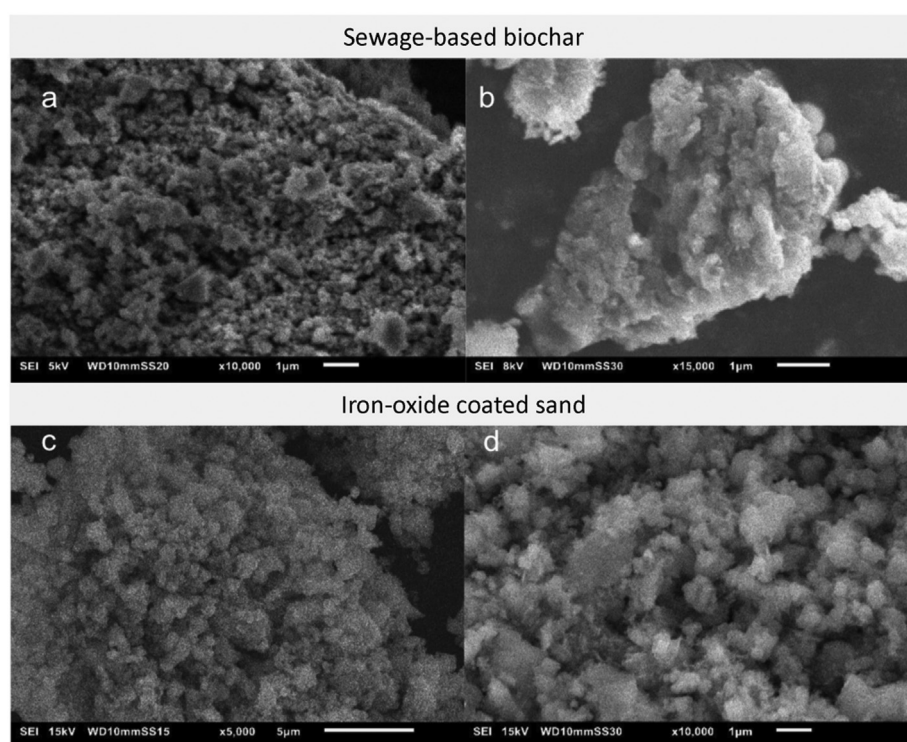

Fig. 4. Scanning electron microscopy images of sewage-sludge biochar at magnifications of (a) 10.000× and (b) 15.000× and iron-oxide-coated sand at (c) 5.000× and (d) 10.000×.
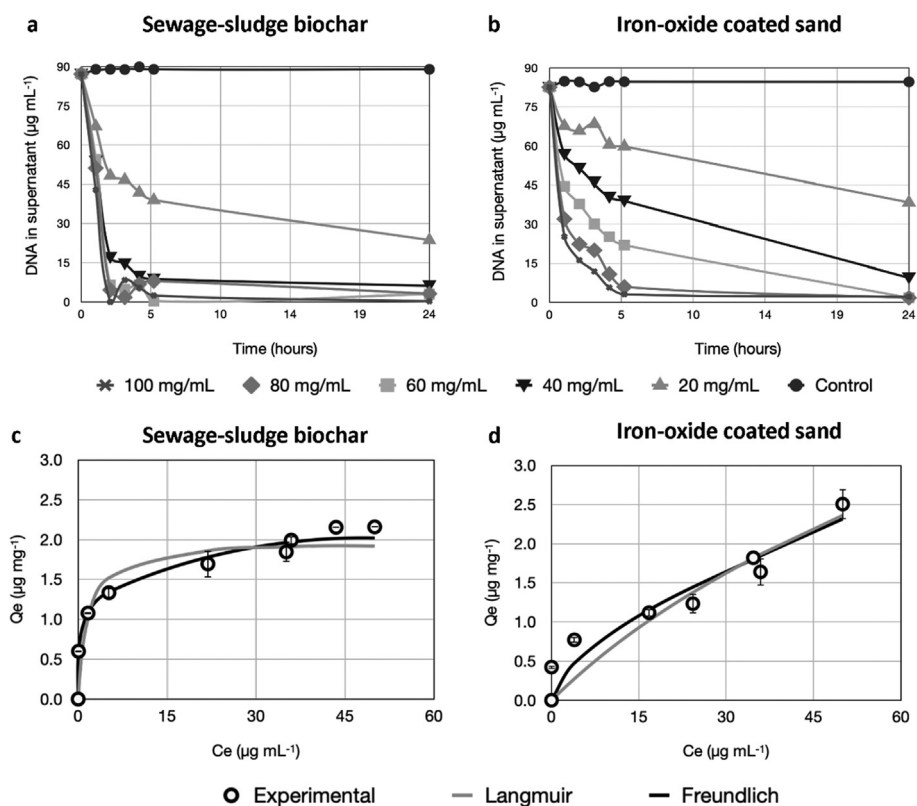
Fig. 5. Equilibrium time of salmon sperm DNA on treated wastewater for (a) sewage sludge biochar and (b) iron oxide coated sands. An initial DNA concentration of 100 µg mL^{-1} was used with the adsorbent ranging from 0 to 100 mg mL^{-1}. Freundlich and Langmuir isotherms models were fitted from experimental data in ultrapure water on (c) sewage-sludge biochar and (d) iron-oxide-coated sand. The equilibrium salmon sperm DNA concentration (Ce; a–b) and the amount of salmon sperm DNA adsorbed per unit of adsorbent (Qe; c–d) are displayed on the graphs.

(depending on flow rates of 0.1–0.5 mL min^{-1}) higher (more time needed to get saturated) on sewage-sludge biochar than iron-oxide-coated sand. With filtered WWTP effluent water, the breakthrough point of sewage-sludge biochar was 4.2 ± 1.8 times (depending on initial DNA concentrations) and 4.6 ± 1.3 times (depending on flow rates) higher than iron-oxide-coated sand. The details on breakthrough points are delivered in Table S5 in Supplementary information.

The Thomas and Yoon-Nelson mathematical models were used to evaluate the effect of process variables on the efficiency of DNA adsorption in the packed-bed columns (Table S6). The two models are mathematically equivalent (Chu, 2020). The only difference between the model is the definition of their variables. Thomas model is used to estimate the absorptive capacity of the adsorbent while the Yoon-Nelson is

used to predict the run time before regeneration or replacement of the column is needed.

The Thomas model was used to analyze the DNA breakthrough curves on sewage-sludge biochar and iron-oxide-coated sand on different water qualities. The Thomas model constant K_{TH} increased with the flow rate for both materials and both water qualities. The adsorption capacity at equilibrium q_e was close to experimental results ($q_{e\ (exp)}$), especially on ultrapure water. Thomas model adequately described the experimental breakthrough data. This indicates that external and internal diffusions are not the only rate-limiting steps in the DNA adsorption process.

The Yoon-Nelson model was applied to determine how much time could the adsorbents be used for DNA removal. According to the
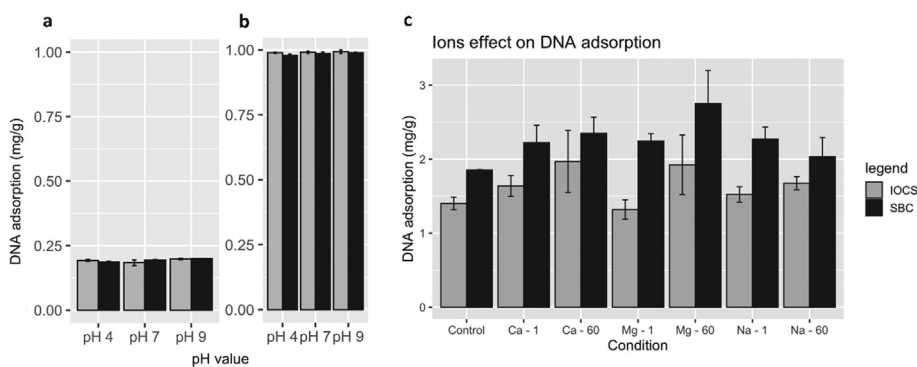
Fig. 6. The influence of pH on DNA adsorption (mg DNA g material $^{-1}$) by sewage-sludge biochar (SBC) and iron-oxide-coated sands (IOCS). The initial concentration of DNA was 20 mg L^{-1} (A) and 100 mg L^{-1} (B), respectively. No significant difference ($p < 0.05$) among treatments was observed. (C) The influence of Ca^{+2}, Mg^{2+} and Na$^+$ on adsorption of DNA (100 mg L^{-1}) on sewage-sludge biochar (SBC) and iron-oxide-coated sands (IOCS). DNA adsorption stands for mg of DNA per g of adsorbent added. The concentrations of the ions were set at 1 and 60 mmol L^{-1}. Significant difference is defined by (*) when $p < 0.05$.
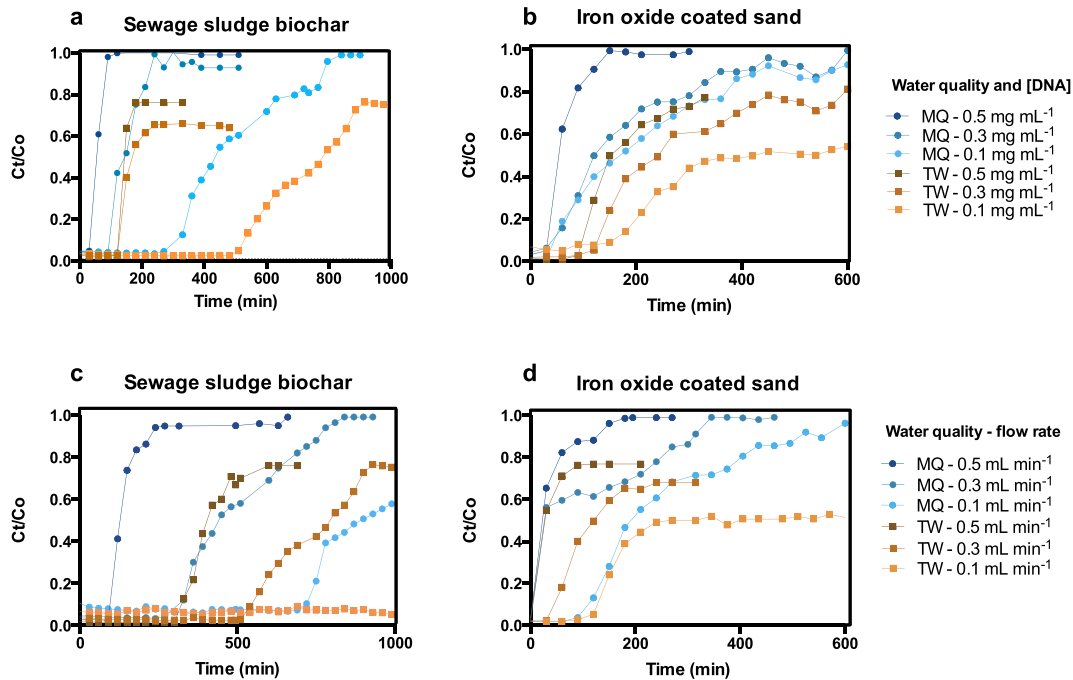
Fig. 7. Experimental breakthrough curves for the continuous-flow adsorption of salmon sperm DNA in up-flow packed-bed columns filled with sewage-sludge biochar (a, c) and iron-oxide-coated sand (b, d) adsorbents. The effect of the initial DNA concentration (0.1–0.5 mg DNA mL^{-1}) was tested at a flow rate of 0.1 mL min^{-1} of either ultrapure water (MilliQ, MQ; *blue curves*) or filtered WWTP effluent water (treated wastewater, TW; *brown curves*). The effect of the flow rate (0.1–0.5 mL min^{-1}) was tested at an initial DNA concentration of 0.3 mg DNA mL^{-1}. (For interpretation of the references to colour in this figure legend, the reader is referred to the web version of this article.)

interpolation of the model plot, the Yoon-Nelson model constant K_{YN} increased with the inlet DNA concentration. The breakthrough time τ decreased with increasing flow rate and initial DNA concentration: the column saturated faster because of less contact time and higher number of DNA molecules to be adsorbed. The small differences between experimental and predicted τ values indicated that Yoon-Nelson model gave an appropriate fit to the experimental column data on continuous DNA adsorption.

3.5. Humic acids interfere on DNA adsorption with effluent water matrices

With ultrapure water, both sewage-sludge biochar and iron-oxide-coated sand were fully saturated by salmon sperm DNA (ratio Ct/$C_o \approx 1$) in column studies. This exhaustion point could not be achieved with filtered WWTP effluent water (Fig. 7). The effect of water qualities was explained by the interaction/adsorption of DNA on organic

components of the filtered WWTP effluent water like humic acids (HAs) that are absent in ultrapure water. If DNA added in the inlet binds to organic components such as humic acids and adsorbs onto biochar, the detection of the DNA concentration that was supposed to be in the eluent will be compromised.

HAs are important components of soils and natural waters, that are formed during humification of organic matter by microorganisms and that bind metal ions in these environmental systems (Kochany and Smith, 2001). We incubated salmon sperm DNA and the adsorbents with a range of HAs concentrations (0 to 100 mg HAs L^{-1}) to assess their influence on DNA adsorption in batches.

Increasing HAs concentrations resulted in a significant decrease in the DNA adsorption capacity of the sewage-sludge biochar (Δ0.5 mg DNA g HA^{-1}, 90.5% decrease) and iron-oxide-coated sand (Δ0.12 mg DNA g HA^{-1}, 17% decrease) (Fig. 8). When only HAs were supplied, DNA adsorbed onto them (0.42 mg g^{-1}). Saeki et al. (2011) showed a similar effect when DNA molecules were exposed to HAs, suggesting that HAs can adsorb and fix DNA. HAs can also directly adsorb onto biochar (Feng et al., 2008), thus enhancing the DNA binding capacity of the biochar. This can explain why the DNA concentration in the column outlet never reached the inlet DNA concentration when the adsorbents in the columns were DNA-saturated.
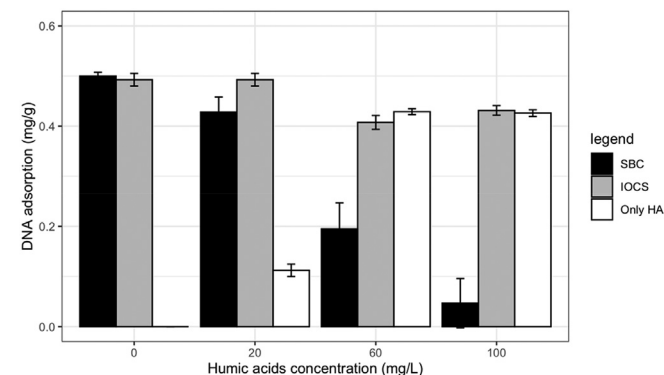
3.6. More than 95% of ARGs and MGEs present in the environmental DNA were removed by sewage-sludge biochar in up-flow column

The removal of ARGs and MGEs from 1 L of WWTP effluent water was assessed in the two up-flow packed-bed columns filled with sewage-sludge biochar and iron-oxide-coated sand. Experiments were conducted both with raw (*i.e.*, unfiltered) and 0.2-μm filtered WWTP effluent water in order to differentiate between the removals of the xenogenetic elements from the total environmental DNA (*i.e.*, sum of free-floating extracellular DNA and microorganisms with their intracellular DNA) and the free-floating exDNA fraction. qPCR was used to quantify the concentrations of ARG and MGE copies from a representative panel of genes for the Netherlands.

Fig. 8. Influence of humic acids (HAs) on DNA adsorption on sewage-sludge biochar (SBC), iron-oxide-coated sands (IOCS) and only HAs. Salmon sperm DNA was used as a DNA template at a concentration of 20 μg mL^{-1}. DNA adsorption stands for mg of DNA per g of adsorbent added.
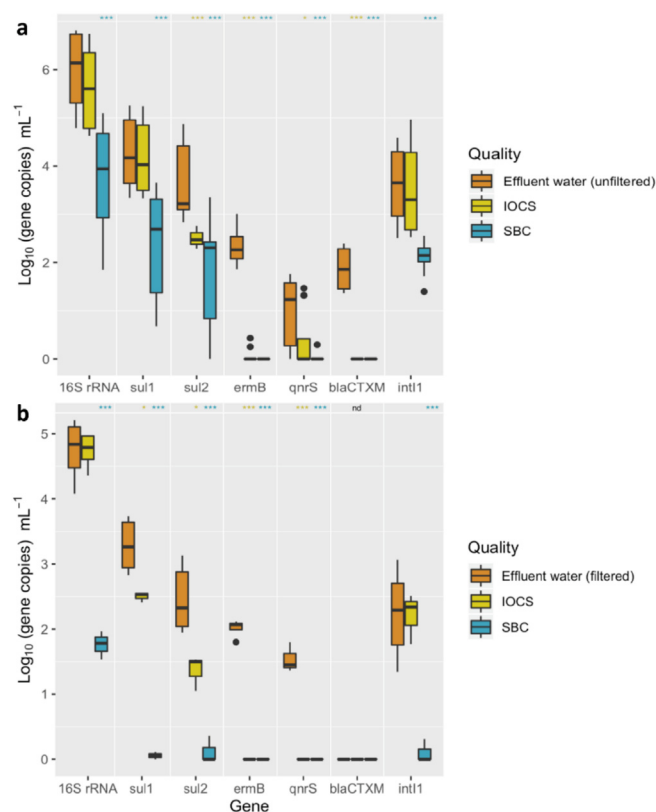
Fig. 9. Quantitative PCR results assessing differences in the concentrations of ARGs and MGE in the unfiltered (a) and filtered (b) WWTP effluent and in the outlet stream of the adsorption columns filled with either iron-oxide-coated sand (IOCS) orsewage-sludge biochar (SBC). (a) Comparison was done with unfiltered effluent water samples assessing the removal of environmental DNA (*i.e.*, including both free-floating exDNA and antibiotic resistantant bacteria). (b) Comparison was done with filtered effluent water samples assessing the free-floating exDNA removal (*i.e.*, in absence of microorganisms). Values are shown on Log$_{10}$ gene copies mL^{-1} from a panel of 16S rRNA gene, selected ARGs (*sul1, sul2, ermB, qnrS and bla$_{CTXM}$*) and one MGE (*intI1*). Statistical significance: p < 0.05(*), p < 0.005 (**), p < 0.0005 (***). Note: "nd" stands for "non-detected". Black dots represent data outliers.

With unfiltered WWTP effluent water (Fig. 9a, Table 4), it was observed that all the tested genes in the sewage-sludge biochar eluent were significantly reduced (*p* < 0.0005) when compared with their inlet concentration (log$_{10}$ gene copies mL^{-1}). Regarding the iron-oxide coated sands eluent, only *sul2, ermB*, and *bla$_{CTXM}$* was significantly reduced (p < 0.0005) and *qnrS* (*p* < 0.05) when compared from their inlet concentrations. Individual qPCR gene values per sample are listed in Table S7.

With filtered WWTP effluent water (Fig. 9b, Table 4), all the tested genes in the sewage-sludge biochar eluent were significantly reduced when compared with the inlet filtered treated wastewater (p < 0.0005), especially *qnrS, ermB* and *bla$_{ctxm}$* that were no longer detected in the column eluent. Regarding iron-oxide coated sands, only *sul1* and *sul2* (p < 0.05) and *ermB* and *qnrS* (p < 0.0005) were significantly reduced in the eluent when compared with the column inlet concentrations. Individual qPCR gene values per sample are listed in Table S8 in Supplementary information.

Overall, 97% and 66% of the targeted genes present in the total environmental DNA of the raw WWTP effluent water decreased from the inlet to the outlet of the sewage-sludge biochar and iron-oxide-coated sand columns, respectively. During experiments conducted with filtered WWTP effluent water, the genes were removed at 85% and 54% by retention of the free-floating exDNA in the sewage-sludge biochar and iron-oxide-coated sand columns, respectively. Individual removal values per gene are listed in Table S9 in Supplementary information.

Table 2
Physicochemical properties and elemental compositions of sewage-sludge biochar prepared by pyrolysis at 600 °C of surplus activated sludge obtained from a WWTP and of iron-oxide-coated sand reclaimed from a drinking WTP.

Parameter	Sewage-sludge biochar	Iron-oxide-coated sand
Physicochemical properties		
Production yield (%)	38.6	–
Moisture content initial (%)	78.9	–
Moisture content final (%)	6.1	
Volatile matter (%)	68.1	–
Surface area (m^{2}g^{-1})	32.4	164.9
Pore diameter (nm)	10.1	6.2
pH (−)	8.0	8.2
Elemental composition (%)		
C	14.1	2.1
H	1.7	3.3
O	37.4[a]	43.7[a]
N	1.9	0.01
S	19.5	–
P	7.7	–
Ca	4.3	–
Mg	5.6	–
Fe	3.9	27.3
Si	3.2	23.6
Al	1.3	–

[a] Oxygen content estimation.

3.7. Outlook: valorizing surplus sludge as biochar to mitigate ARG levels in WWTP effluents

We highlighted that materials reclaimed from wastes of water engineering facilities, namely WWTP and drinking WTP, can become effective adsorbents to remove ARGs and MGEs from WWTP effluents. We involved a detailed examination of both the free-floating exDNA fraction and the total environmental DNA.

Sewage-sludge biochar produced by pyrolysis of surplus sewage sludge is an attractive, reclaimed and low-cost alternative to manufactured powdered activated carbon for the removal of xenogenetic elements from wastewater by adsorption. Adsorption capacity similar to activated carbon was obtained with sewage-sludge biochar in batch tests. We acknowledge that biochar can be more variable in composition and properties than activated carbon due to the type of sludge and pyrolysis conditions. Before going for full-scale operation, the variability of adsorption properties of biochar needs to be checked depending on biomasses and conditions used for production. Further studies can be conducted to investigate this important aspect using multifactorial experimental design. Biochar is widely used worldwide for sanitation. Numerous studies have highlighted biochar as a very effective material to remove antibiotics, heavy metals, and resistance (Aly, 2016; Fu et al., 2021; Tian et al., 2019). Besides high-grade technological solutions for industrialized countries, we need to bring science into low-cost scalable and implementable solutions for regions with less access to expensive technologies.

Sewage sludge surplus in WWTPs gradually increase with the rising world population and the needs for sanitation and installation of new WWTPs thereof. At European level, sludge production reaches 13 million tons by 2020 (Capodaglio and Callegari, 2018). The treatment and discarding of sewage sludge (*e.g.*, landfilling, agriculture and incineration) is an expensive and ecological burden. The European directive 86/278/EEC on agricultural use of sewage sludge set stringent regulations because of the presence of high concentrations of heavy metals and pathogens. Incineration is carried out in most of EU-15 countries, like the Netherlands (Agrafioti et al., 2013; Capodaglio and Callegari, 2018). Large-scale incineration requires high investment and operating costs together with extensive cleaning and gas purification.

Pyrolysis can become an interesting alternative to reduce sludge volumes, remove pathogens, and simultaneously convert the sludge organic matter into biofuel or biochar (Inguanzo et al., 2002). In contrast to incineration, pyrolysis requires less or no oxygen and eventually

Table 3
Parameters derived from Freundlich (Eq. (2)) and Langmuir (Eq. (3)) isotherm models calibrated to the DNA adsorption profiles onto sewage-sludge biochar and iron-oxide-coated sand materials in ultrapure water and filtered (0.2 μm) WWTP effluent water.

Adsorbent	Type of water	Freundlich multilayer isotherm model				Langmuir monolayer Isotherm model		
		R^2 (−)	K_F (mg DNA g^{-1} adsorbent)	1/n (−)	n (−)	R^2 (−)	q_{max} (mg DNA g^{-1} adsorbent)	K_L (L mg^{-1} DNA)
Sewage-sludge biochar	Ultrapure water	0.95	1.4	0.13	7.87	0.89	2.2	1.81
	Filtered WWTP effluent water	0.99	1.0	0.19	5.16	0.92	2.0	0.61
Iron-oxide-coated sand	Ultrapure water	0.81	0.3	0.31	3.20	0.78	1.7	0.06
	Filtered WWTP effluent water	0.93	0.21	0.61	1.63	0.89	5.8	0.01

reduces the generation of flue and acid gases to be cleaned (Hwang et al., 2007). Pyrolysis can also be interestingly driven in solar furnaces (Ayala-Cortés et al., 2019), minimizing energetic costs. Biochar produced out of dewatered sewage-sludge can efficiently remove chemical pollutants from wastewater (Fathi Dokht et al., 2017) like agrichemicals, pharmaceuticals, personal care products or endocrine disrupting compounds (Thompson et al., 2016). The here-demonstrated ability of sewage-sludge biochar to remove nucleic acids and their problematic xenogenetic contents is an asset, besides promoting circularity in water resource factories.

Finally, exDNA free-floats in typical concentrations of 5.6 $\pm$ 2.9 μg L^{-1} in effluent wastewater (Calderón-Franco et al., 2020b). The here-sampled WWTP treats 200′000 m^3 day^{-1}, corresponding to a discharge of 1 kg exDNA day^{-1}. Since removing up to more than 85% of the free-floating genes, a sewage-sludge biochar solution can prevent the discharge of 310 kg exDNA year^{-1} on top of problematic microorganisms within the environmental DNA released from the catchment area of this largest WWTP of the Netherlands.

4. Conclusion

We showed the potential of waste materials from WWTPs and drinking WTPs like surplus activated sludge and used iron-oxide-coated sand to get revalorized to remove free-floating exDNA and total environmental DNA containing ARGs and MGEs from treated wastewater. The main conclusions of this work are:

1. Sewage-sludge biochar displayed physical-chemical characteristics and DNA adsorption efficiencies similar to powdered activated carbon. Sewage-sludge biochar can be efficiently implemented in batches or continuous-flow packed-bed systems. Further multifactorial studies should address the variability in product characteristics and adsorption capacities of biochars.
2. The removal of ARGs and MGEs was remarkable, notably with sewage-sludge biochar. From the total environmental DNA (*i.e.*, composed of both intracellular and extracellular DNAs), 97% of the evaluated genes were adsorbed and removed from raw unfiltered WWTP effluent water in continuous-flow packed-bed columns filled with sewage-sludge biochar while a 66% removal was achieved with iron-oxide-coated sand. From the free-floating exDNA fraction, 85% of ARGs and MGEs were retained with this exDNA fraction in the sewage-sludge biochar column; 54% with iron-oxide-coated sand.

3. Recycling surplus sludge and other waste biomasses into a low-cost, scalable and implementable solution can help remove the load of AMR released in aquatic environments.

By aligning to UN SDGs for clean water & sanitation and responsible consumption & production, we provide here a solution to mitigate the emission of problematic xenogenetic elements from sewage into surface waters. Both end-of-pipe but also decentralized technologies can be developed from this science-based evidence to remove AMR from used water streams at low cost.

CRediT authorship contribution statement

DCF and SA designed the study with DGW, and additional input from MvL on adsorbent selection. DCF and AS performed the experimental investigations. DCF, SA and DGW critically assessed the experiments, data, and scientific findings. DCF wrote the manuscript with direct contribution, edits, and critical feedback by all authors. DCF and SA are first co-authors of this manuscript.

Declaration of competing interest

The authors declare no conflict of interest.

Acknowledgements

Table 4
Quantitative PCR results assessing the 16S rRNA gene, a panel of antibiotic resistance genes, and the integrase I class 1 as a mobile genetic element. Values represent the log$_{10}$ gene copies differences between the inlet (unfiltered or filtered effluent water) and outlet of the adsorption columns tested with either iron-oxide-coated sand or sewage-sludge biochar.

Type of water	Material	ΔGene (log$_{10}$ gene copies differences inlet-outlet)						
		16S rRNA	sul1	sul2	ermB	qnrS	bla$_{ctxm}$	intl1
Unfiltered effluent water	Iron-oxide-coated sand	0.34 $\pm$ 1.1	0.1 $\pm$ 1.0	1.2 $\pm$ 0.8	2.3 $\pm$ 0.4	0.7 $\pm$ 0.8	1.9 $\pm$ 0.4	0.1 $\pm$ 1.2
	Sewage-sludge biochar	2.3 $\pm$ 1.4	1.9 $\pm$ 1.3	1.8 $\pm$ 1.3	2.4 $\pm$ 0.4	1.0 $\pm$ 0.7	1.9 $\pm$ 0.4	1.5 $\pm$ 0.8
Filtered effluent water	Iron-oxide-coated sand	0.003 $\pm$ 0.5	0.8 $\pm$ 0.4	1.1 $\pm$ 0.5	2.1 $\pm$ 0.02	1.4 $\pm$ 0.04	0	0.03 $\pm$ 0.7
	Sewage-sludge biochar	3.0 $\pm$ 0.5	3.2 $\pm$ 0.4	2.3 $\pm$ 0.5	2.1 $\pm$ 0.03	1.4 $\pm$ 0.05	0	2.1 $\pm$ 0.6

Appendix A. Supplementary data

Supplementary data to this article can be found online at https://doi.org/10.1016/j.scitotenv.2021.146364.

References

Agrafioti, E., Bouras, G., Kalderis, D., Diamadopoulos, E., 2013. Biochar production by sewage sludge pyrolysis. J. Anal. Appl. Pyrolysis 101, 72–78. https://doi.org/10.1016/j.jaap.2013.02.010.

Aly, H.M., 2016. Short communication: biochar and its importance in adsorption of antibiotic and heavy metals from aqueous solutions. Ecol. Quest. 24, 75–78. doi:10.12775/EQ.2016.014.

Ayala-Cortés, A., Arancibia-Bulnes, C.A., Villafán-Vidales, H.I., Lobato-Peralta, D.R., Martínez-Casillas, D.C., Cuentas-Gallegos, A.K., 2019. Solar pyrolysis of agave and tomato pruning wastes: insights of the effect of pyrolysis operation parameters on the physicochemical properties of biochar. AIP Conf. Proc. 2126. https://doi.org/10.1063/1.5117681.

Cacace, D., Fatta-Kassinos, D., Manaia, C.M., Cytryn, E., Kreuzinger, N., Rizzo, L., Karaolia, P., Schwartz, T., Alexander, J., Merlin, C., Garelick, H., Schmitt, H., de Vries, D., Schwermer, C.U., Meric, S., Ozkal, C.B., Pons, M.N., Kneis, D., Berendonk, T.U., 2019. Antibiotic resistance genes in treated wastewater and in the receiving water bodies: a pan-European survey of urban settings. Water Res. 162, 320–330. https://doi.org/10.1016/j.watres.2019.06.039.

Cai, P., Huang, Q.-Y., Zhang, X.-W., 2006a. Interactions of DNA with clay minerals and soil colloidal particles and protection against degradation by DNase. Environ. Sci. Technol. 40, 2971–2976. https://doi.org/10.1021/es0522985.

Cai, P., Huang, Q., Jiang, D., Rong, X., Liang, W., 2006b. Microcalorimetric studies on the adsorption of DNA by soil colloidal particles. Colloids Surfaces B Biointerfaces 49, 49–54. https://doi.org/10.1016/j.colsurfb.2006.02.011.

Cai, P., Huang, Q., Zhang, X., Chen, H., 2006c. Adsorption of DNA on clay minerals and various colloidal particles from an Alfisol. Soil Biol. Biochem. 38, 471–476. https://doi.org/10.1016/j.soilbio.2005.05.019.

Calderón-Franco, D., Lin, Q., Van Loosdrecht, M.C.M., Abbas, B., Weissbrodt, D.G., 2020a. Anticipating xenogenic pollution at the source: impact of sterilizations on DNA release from microbial cultures. Front. Bioeng. Biotechnol. 8, 1–13. https://doi.org/10.3389/fbioe.2020.00171.

Calderón-Franco, D., van Loosdrecht, M., Abeel, T., Weissbrodt, D., 2020b. Free-floating extracellular DNA: systematic profiling of mobile genetic elements and antibiotic resistance from wastewater. Water Res. 189, 1–13. https://doi.org/10.1101/2020.05.01.072397.

Capodaglio, A.G., Callegari, A., 2018. Feedstock and process influence on biodiesel produced from waste sewage sludge. J. Environ. Manag. 216, 176–182. https://doi.org/10.1016/j.jenvman.2017.03.089.

Chatterjee, S., Mondal, S., De, S., 2018. Design and scaling up of fixed bed adsorption columns for lead removal by treated laterite. J. Clean. Prod. 177, 760–774. https://doi.org/10.1016/j.jclepro.2017.12.249.

Chen, S., Yue, Q., Gao, B., Li, Q., Xu, X., Fu, K., 2012. Bioresource technology adsorption of hexavalent chromium from aqueous solution by modified corn stalk : a fixed-bed column study. Bioresour. Technol. 113, 114–120. https://doi.org/10.1016/j.biortech.2011.11.110.

Cheng, X., Delanka-Pedige, H.M.K., Munasinghe-Arachchige, S.P., Abeysiriwardana-Arachchige, I.S.A., Smith, G.B., Nirmalakhandan, N., Zhang, Y., 2020. Removal of antibiotic resistance genes in an algal-based wastewater treatment system employing Galdieria sulphuraria: a comparative study. Sci. Total Environ. 711, 134435. https://doi.org/10.1016/j.scitotenv.2019.134435.

Chowdhury, Z.Z., Abd Hamid, S.B., Zain, S.M., 2015. Evaluating design parameters for breakthrough curve analysis and kinetics of fixed bed columns for Cu(II) cations using lignocellulosic wastes. BioResources 10, 732–749. doi:10.15376/biores.10.1.732-749.

Chu, K.H., 2020. Breakthrough curve analysis by simplistic models of fixed bed adsorption: in defense of the century-old Bohart-Adams model. Chem. Eng. J. 380, 122513. https://doi.org/10.1016/j.cej.2019.122513.

Czekalski, N., Berthold, T., Caucci, S., Egli, A., Bürgmann, H., 2012. Increased levels of multiresistant bacteria and resistance genes after wastewater treatment and their dissemination into Lake Geneva. Switzerland. Front. Microbiol. 3, 1–18. https://doi.org/10.3389/fmicb.2012.00106.

Daful, A.G., R Chandraratne, M., 2018. Biochar production from biomass waste-derived material, Reference Module in Materials Science and Materials Engineering. Elsevier Ltd. doi:https://doi.org/10.1016/b978-0-12-803581-8.11249-4.

Dai, Z., Webster, T.M., Enders, A., Hanley, K.L., Xu, J., Thies, J.E., Lehmann, J., 2017. DNA extraction efficiency from soil as affected by pyrolysis temperature and extractable organic carbon of high-ash biochar. Soil Biol. Biochem. 115, 129–136. https://doi.org/10.1016/j.soilbio.2017.08.016.

Desta, M.B., 2013. Batch sorption experiments: Langmuir and freundlich isotherm studies for the adsorption of textile metal ions onto teff straw (eragrostis tef) agricultural waste. J. Thermodyn. 1. https://doi.org/10.1155/2013/375830.

Destiani, R., Templeton, M.R., 2019. Chlorination and ultraviolet disinfection of antibiotic-resistant bacteria and antibiotic resistance genes in drinking water. AIMS Environ. Sci. 6, 222–241. https://doi.org/10.3934/environsci.2019.3.222.

Eggen, R.I.L., Hollender, J., Joss, A., Schärer, M., Stamm, C., 2014. Reducing the discharge of micropollutants in the aquatic environment: the benefits of upgrading wastewater treatment plants. Environ. Sci. Technol. 48, 7683–7689. https://doi.org/10.1021/es500907n.

Fang, J., Jin, L., Meng, Q., Wang, D., Lin, D., 2021. Interactions of extracellular DNA with aromatized biochar and protection against degradation by DNase I. J. Environ. Sci. (China) 101, 205–216. https://doi.org/10.1016/j.jes.2020.08.017.

Fathi Dokht, H., Movahedi Naeini, S.A., Dordipour, E., De Jong, L.W., Hezarjaribi, E., 2017. Effects of sewage sludge and its biochar on soybean yield in fine-textured loess soil. Environ. Heal. Eng. Manag. 4, 81–91. doi:10.15171/ehem.2017.12.

Feng, H.J., Hu, L.F., Mahmood, Q., Long, Y., Shen, D.S., 2008. Study on biosorption of humic acid by activated sludge. Biochem. Eng. J. 39, 478–485. https://doi.org/10.1016/j.bej.2007.11.004.

Fu, Y., Wang, F., Sheng, H., Hu, F., Wang, Z., Xu, M., Bian, Y., Jiang, X., Tiedje, J.M., 2021. Removal of extracellular antibiotic resistance genes using magnetic biochar/quaternary phosphonium salt in aquatic environments: a mechanistic study. J. Hazard. Mater. 411, 125048. https://doi.org/10.1016/j.jhazmat.2021.125048.

Gillings, M.R., Westoby, M., Ghaly, T.M., 2018. Pollutants that replicate: xenogenetic DNAs. Trends Microbiol. 26, 975–977. https://doi.org/10.1016/j.tim.2018.08.003.

Gould, I.M., Bal, A.M., Gould, I.M., Bal, A.M., 2015. New antibiotic agents in the pipeline and how they can help overcome microbial resistance New antibiotic agents in the pipeline and how they can help overcome microbial resistance 5594, 185–191. doi:10.4161/viru.22507.

Grehs, B.W.N., Lopes, A.R., Moreira, N.F.F., Fernandes, T., Linton, M.A.O., Silva, A.M.T., Manaia, C.M., Carissimi, E., Nunes, O.C., 2019. Removal of microorganisms and antibiotic resistance genes from treated urban wastewater: A comparison between aluminium sulphate and tannin coagulants. Water Res., 166 https://doi.org/10.1016/j.watres.2019.115056.

Han, R., Wang, Yu, Zhao, X., Wang, Yuanfeng, Xie, F., Cheng, J., Tang, M., 2009. Adsorption of methylene blue by phoenix tree leaf powder in a fixed-bed column: experiments and prediction of breakthrough curves. Desalination 245, 284–297. doi:https://doi.org/10.1016/j.desal.2008.07.013.

Huang, Y., Yang, J.K., Keller, A.A., 2014. Removal of arsenic and phosphate from aqueous solution by metal (hydr-)oxide coated sand. ACS Sustain. Chem. Eng. 2, 1128–1138. https://doi.org/10.1021/sc400484s.

Hwang, I.H., Ouchi, Y., Matsuto, T., 2007. Characteristics of leachate from pyrolysis residue of sewage sludge. Chemosphere 68, 1913–1919. https://doi.org/10.1016/j.chemosphere.2007.02.060.

Inguanzo, M., Domínguez, A., Menéndez, J., Blanco, C.G., Pis, J.J., 2002. On the pyrolysis of sewage sludge: the influence of pyrolysis conditions on solid, liquid and gas fractions. J. Anal. Appl. Pyrolysis 63, 209–222. https://doi.org/10.1016/S0165-2370(01)00155-3.

Kappell, A.D., Kimbell, L.K., Seib, M.D., Carey, D.E., Choi, M.J., Kalayil, T., Fujimoto, M., Zitomer, D.H., McNamara, P.J., 2018. Removal of antibiotic resistance genes in an anaerobic membrane bioreactor treating primary clarifier effluent at 20 °C. Environ. Sci. Water Res. Technol. 4, 1783–1793. https://doi.org/10.1039/c8ew00270c.

Karkman, A., Do, T.T., Walsh, F., Virta, M.P.J., 2018. Antibiotic-resistance genes in waste water. Trends Microbiol. 26, 220–228. https://doi.org/10.1016/j.tim.2017.09.005.

Kochany, J., Smith, W., 2001. Application of Humic Substances in Environmental Remediation. Appl. humic Subst. Environ, Remediat.

Krzemiński, P., Popowska, M., 2020. Treatment Technologies for Removal of Antibiotics, Antibiotic Resistance Bacteria and Antibiotic-Resistant Genes, Antibiotics and Antimicrobial Resistance Genes. Emerging Contaminants and Associated Treatment Technologies. Springer, Cham. Springer, Cham. doi:10.1007/978-981-13-1577-0_11.

Lee Ventola, C. 2015. Antibiotic resistance crisis. P&T a peer-reviewed J. Formul. Manag. 40, 277–83.

Leite, D.C.A., Balieiro, F.C., Pires, C.A., Madari, B.E., Rosado, A.S., Coutinho, H.L.C., Peixoto, R.S., 2014. Comparison of DNA extraction protocols for microbial communities from soil treated with biochar. Brazilian J. Microbiol. 45, 175–183. https://doi.org/10.1590/S1517-83822014000100023.

Li, N., Sheng, G.P., Lu, Y.Z., Zeng, R.J., Yu, H.Q., 2017. Removal of antibiotic resistance genes from wastewater treatment plant effluent by coagulation. Water Res. 111, 204–212. https://doi.org/10.1016/j.watres.2017.01.010.

Lu, X., Zhang, X.X., Wang, Z., Huang, K., Wang, Y., Liang, W., Tan, Y., Liu, B., Tang, J., 2015. Bacterial pathogens and community composition in advanced sewage treatment systems revealed by metagenomics analysis based on high-throughput sequencing. PLoS One 10, 1–15. https://doi.org/10.1371/journal.pone.0125549.

Ma, L., Li, A.D., Le Yin, X., Zhang, T., 2017. The prevalence of integrons as the carrier of antibiotic resistance genes in natural and man-made environments. Environ. Sci. Technol. 51, 5721–5728. https://doi.org/10.1021/acs.est.6b05887.

Mao, D., Luo, Y., Mathieu, J., Wang, Q., Feng, L., Mu, Q., Feng, C., Alvarez, P.J.J., 2014. Persistence of extracellular DNA in river sediment facilitates antibiotic resistance gene propagation. Environ. Sci. Technol. 48, 71–78. https://doi.org/10.1021/es404280v.

McEachran, A.D., Hedgespeth, M.L., Newton, S.R., McMahen, R., Strynar, M., Shea, D., Nichols, E.G., 2018. Comparison of emerging contaminants in receiving waters downstream of a conventional wastewater treatment plant and a forest-water reuse system. Environ. Sci. Pollut. Res. 25, 12451–12463. https://doi.org/10.1007/s11356-018-1505-5.

Méndez, A., Terradillos, M., Gascó, G., 2013. Physicochemical and agronomic properties of biochar from sewage sludge pyrolysed at different temperatures. J. Anal. Appl. Pyrolysis 102, 124–130. https://doi.org/10.1016/j.jaap.2013.03.006.

Moore, D., Dowhan, D., 2002. Purification and Concentration of DNA. Curr. Protoc. Mol, Biol.

Naderi, M., 2015. Surface Area: Brunauer-Emmett-Teller (BET). Prog. Filtr. Sep. 585–608. https://doi.org/10.1016/B978-0-12-384746-1.00014-8.

Ngigi, A.N., Ok, Y.S., Thiele-Bruhn, S., 2020. Biochar affects the dissipation of antibiotics and abundance of antibiotic resistance genes in pig manure. Bioresour. Technol. 315, 123782. https://doi.org/10.1016/j.biortech.2020.123782.

Nguyen, T.H., Chen, K.L., 2007. Role of divalent cations in plasmid DNA adsorption to natural organic matter-coated silica surface. Environ. Sci. Technol. 41, 5370–5375. https://doi.org/10.1021/es070425m.

Pallares-Vega, R., Blaak, H., van der Plaats, R., de Roda Husman, A.M., Hernandez Leal, L., van Loosdrecht, M.C.M., Weissbrodt, D.G., Schmitt, H., 2019. Determinants of presence and removal of antibiotic resistance genes during WWTP treatment: a cross-sectional study. Water Res. 161, 319–328. https://doi.org/10.1016/j.watres.2019.05.100.

Pazda, M., Kumirska, J., Stepnowski, P., Mulkiewicz, E., 2019. Antibiotic resistance genes identified in wastewater treatment plant systems – a review. Sci. Total Environ. https://doi.org/10.1016/j.scitotenv.2019.134023.

Pruden, A., Pei, R., Storteboom, H., Carlson, K.H., 2006. Antibiotic resistance genes as emerging contaminants: studies in northern Colorado. Environ. Sci. Technol. 40, 7445–7450. https://doi.org/10.1021/es060413l.

Riquelme Breazeal, M.V., Novak, J.T., Vikesland, P.J., Pruden, A., 2013. Effect of wastewater colloids on membrane removal of antibiotic resistance genes. Water Res. 47, 130–140. https://doi.org/10.1016/j.watres.2012.09.044.

Rizzo, L., Krätke, R., Linders, J., Scott, M., Vighi, M., de Voogt, P., 2018. Proposed EU minimum quality requirements for water reuse in agricultural irrigation and aquifer recharge: SCHEER scientific advice. Curr. Opin. Environ. Sci. Heal. https://doi.org/10.1016/j.coesh.2017.12.004.

Roberts, D.A., Cole, A.J., Whelan, A., de Nys, R., Paul, N.A., 2017. Slow pyrolysis enhances the recovery and reuse of phosphorus and reduces metal leaching from biosolids. Waste Manag. 64, 133–139. https://doi.org/10.1016/j.wasman.2017.03.012.

Rouf, S., Nagapadma, M., 2015. Modeling of Fixed Bed Column Studies for Adsorption of Azo Dye on Chitosan Impregnated with a Cationic Surfactant. Int. J. Sci. Eng. Res. 6, 538–544. doi:10.14299/ijser.2015.02.006.

Saeki, K., Kunito, T., 2010. Adsorptions of DNA molecules by soils and variable-charged soil constituents GMOs. Appl. Microbiol. 1, 188–195.

Saeki, K., Ihyo, Y., Sakai, M., Kunito, T., 2011. Strong adsorption of DNA molecules on humic acids. Environ. Chem. Lett. 9, 505–509. https://doi.org/10.1007/s10311-011-0310-x.

Shannon, M.A., Bohn, P.W., Elimelech, M., Georgiadis, J.G., Mariñas, B.J., Mayes, A.M., 2008. Science and technology for water purification in the coming decades. Nature 452, 301–310. https://doi.org/10.1038/nature06599.

Sharma, S.K., 2001. Adsorptive iron removal from groundwater. International Inst. Infrastructural, Hydraul. Environ. Eng. Master the, 39–41.

Song, W., Guo, M., 2012. Quality variations of poultry litter biochar generated at different pyrolysis temperatures. J. Anal. Appl. Pyrolysis 94, 138–145. https://doi.org/10.1016/j.jaap.2011.11.018.

Stange, C., Sidhu, J.P.S., Toze, S., Tiehm, A., 2019. Comparative removal of antibiotic resistance genes during chlorination, ozonation, and UV treatment. Int. J. Hyg. Environ. Health 222, 541–548. https://doi.org/10.1016/j.ijheh.2019.02.002.

Tarelho, L.A.C., Hauschild, T., Vilas-Boas, A.C.M., Silva, D.F.R., Matos, M.A.A., 2019. Biochar from pyrolysis of biological sludge from wastewater treatment. Energy Rep., 22–25 https://doi.org/10.1016/j.egyr.2019.09.063.

Thompson, K.A., Shimabuku, K.K., Kearns, J.P., Knappe, D.R.U., Summers, R.S., Cook, S.M., 2016. Environmental comparison of biochar and activated carbon for tertiary wastewater treatment. Environ. Sci. Technol. 50, 11253–11262. https://doi.org/10.1021/acs.est.6b03239.

Tian, R., Li, C., Xie, S., You, F., Cao, Z., Xu, Z., Yu, G., Wang, Y., 2019. Preparation of biochar via pyrolysis at laboratory and pilot scales to remove antibiotics and immobilize heavy metals in livestock feces. J. Soils Sediments 19, 2891–2902. https://doi.org/10.1007/s11368-019-02350-2.

Titiladunayo, I.F., McDonald, A.G., Fapetu, O.P., 2012. Effect of temperature on biochar product yield from selected lignocellulosic biomass in a pyrolysis process. Waste and Biomass Valorization 3, 311–318. https://doi.org/10.1007/s12649-012-9118-6.

Torti, A., Lever, M.A., Jørgensen, B.B., 2015. Origin, dynamics, and implications of extracellular DNA pools in marine sediments. Mar. Genomics 24, 185–196. https://doi.org/10.1016/j.margen.2015.08.007.

Tripathi, V., Tripathi, P., 2017. Antibiotic Resistance Genes: An Emerging Environmental Pollutant. Environmental Science and Engineering, Subseries: Environmental Science https://doi.org/10.1007/978-3-319-46248-6_9.

UNICEF, WHO, JMP, 2019. Progress on Household Drinking Water, Sanitation and Hygiene 2000–2017, Unicef/Who.

Van Der Hoek, J.P., De Fooij, H., Struker, A., 2016. Wastewater as a resource: strategies to recover resources from Amsterdam's wastewater. Resour. Conserv. Recycl. 113, 53–64. https://doi.org/10.1016/j.resconrec.2016.05.012.

Vermeer, A.W.P., Koopal, L.K., 1998. Adsorption of humic acids to mineral particles. 2. polydispersity effects with polyelectrolyte adsorption. Langmuir 14, 4210–4216. https://doi.org/10.1021/la970836o.

Vermeer, A.W.P., Van Riemsdijk, W.H., Koopal, L.K., 1998. Adsorption of humic acid to mineral particles. 1. Specific and electrostatic interactions. Langmuir 14, 2810–2815. https://doi.org/10.1021/la970624r.

Villarroel-Rocha, J., Barrera, D., Sapag, K., 2014. Introducing a self-consistent test and the corresponding modification in the Barrett, Joyner and Halenda method for pore-size determination. Microporous Mesoporous Mater. 200, 68–78. https://doi.org/10.1016/j.micromeso.2014.08.017.

Wang, C., Wang, T., Li, W., Yan, J., Li, Z., Ahmad, R., Herath, S.K., Zhu, N., 2014. Adsorption of deoxyribonucleic acid (DNA) by willow wood biochars produced at different pyrolysis temperatures. Biol. Fertil. Soils 50, 87–94. https://doi.org/10.1007/s00374-013-0836-0.

Weissbrodt, D., Kovalova, L., Ort, C., Pazhepurackel, V., Moser, R., Hollender, J., Siegrist, H., Mcardell, C.S., 2009. Mass flows of x-ray contrast media and cytostatics in hospital wastewater. Environ. Sci. Technol. 43, 4810–4817. https://doi.org/10.1021/es8036725.

von Wintersdorff, C.J.H., Penders, J., van Niekerk, J.M., Mills, N.D., Majumder, S., van Alphen, L.B., Savelkoul, P.H.M., Wolffs, P.F.G., 2016. Dissemination of antimicrobial resistance in microbial ecosystems through horizontal gene transfer. Front. Microbiol. 7, 173. https://doi.org/10.3389/fmicb.2016.00173.

Wu, M.S., Xu, X., 2019. Inactivation of antibiotic-resistant bacteria by chlorine dioxide in soil and shifts in community composition. RSC Adv. 9, 6526–6532. https://doi.org/10.1039/c8ra07997h.

Yang, Y., Li, B., Zou, S., Fang, H.H.P., Zhang, T., 2014. Fate of antibiotic resistance genes in sewage treatment plant revealed by metagenomic approach. Water Res. 62, 97–106. https://doi.org/10.1016/j.watres.2014.05.019.

Yuan, J.H., Xu, R.K., Zhang, H., 2011. The forms of alkalis in the biochar produced from crop residues at different temperatures. Bioresour. Technol. 102, 3488–3497. https://doi.org/10.1016/j.biortech.2010.11.018.

Yuan, Q. Bin, Guo, M.T., Yang, J., 2015. Fate of antibiotic resistant bacteria and genes during wastewater chlorination: implication for antibiotic resistance control. PLoS One 10, 1–11. https://doi.org/10.1371/journal.pone.0119403.

Zhang, Yongpeng, Niu, Z., Zhang, Ying, Zhang, K., 2018. Occurrence of intracellular and extracellular antibiotic resistance genes in coastal areas of Bohai Bay (China) and the factors affecting them. Environ. Pollut. 236, 126–136. https://doi.org/10.1016/j.envpol.2018.01.033.

Zhou, C.S., Wu, J.W., Dong, L.L., Liu, B.F., Xing, D.F., Yang, S.S., Wu, X.K., Wang, Q., Fan, J.N., Feng, L.P., Cao, G.L., 2020. Removal of antibiotic resistant bacteria and antibiotic resistance genes in wastewater effluent by UV-activated persulfate. J. Hazard. Mater. 388, 122070. https://doi.org/10.1016/j.jhazmat.2020.122070.

Zhou, G., Qiu, X., Wu, X., Lu, S., 2021. Horizontal gene transfer is a key determinant of antibiotic resistance genes profiles during chicken manure composting with the addition of biochar and zeolite. J. Hazard. Mater. 408, 124883. https://doi.org/10.1016/j.jhazmat.2020.124883.